International Journal on Magnetic Particle Imaging
Vol 11, No 1, Suppl 1, Article ID 2503035, 3 Pages

Infinite Science Publishing

Proceedings Article

Dipolar interaction effect on magnetization harmonics in liner chain magnetic nanoparticles

Haochen Zhang[a,*] · Yi Sun[a] · Haozhe Wang[a] · Takashi Yoshida[a]

[a]Department of Electrical and Electrical Engineering, Kyushu University, Fukuoka, Japan
[*]Corresponding author, email: zhang.haochen.048@s.kyushu-u.ac.jp

Abstract

Magnetic nanoparticles (MNPs) have been extensively studied for various bio-applications due to their unique magnetic properties. However, strong dipolar interactions in MNPs can alter these properties. In this work, we investigated the influence of dipolar interactions on the harmonics of magnetization in MNPs through numerical simulations. The simulations were conducted on a linear chain of MNPs using the stochastic Landau-Lifshitz-Gilbert equation. The results reveal that, unlike the fundamental magnetization component, the third harmonic component is not solely determined by the magnitude of the dipole interaction field. Instead, it is strongly influenced by the phase lag between the external field and the dipole interaction field.

I. Introduction

Magnetic nanoparticles (MNPs), which are a type of nanoparticles that compatible with human body, have been widely studied for biomedical applications such as hyperthermia and magnetic particle imaging (MPI) [1].

Tay et al. investigated the magnetization properties of the liner chain MNPs (CMNP), which has 10-fold better image resolution and 40-fold stronger signal intensity than conventional MNPs in MPI owing to the step-like *M*–*H* curve [2]. In this study, we investigated the effects of dipole-interaction magnetic field in CMNP on the magnetization harmonics by stochastic Landau-Lifshitz-Gilbert (LLG) equation.

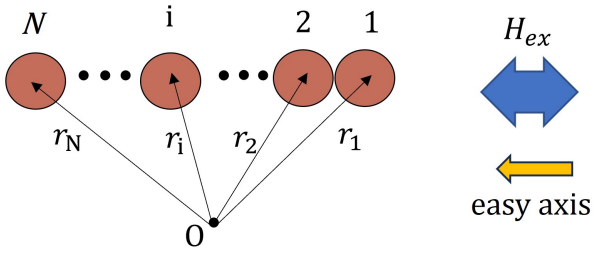

Figure 1: Structure of a CMNP.

II. Model

The dynamics of the magnetization of MNPs are described by the stochastic LLG equation [3]:

$$d\mathbf{u}_i/dt = \mu_0\gamma\mathbf{u}_i \times \left(\mathbf{H}_{\text{eff},i} - \lambda\mathbf{u}_i \times \mathbf{H}_{\text{eff},i}\right), \quad (1)$$

where γ is the gyromagnetic ratio, λ is a dimensionless damping coefficient, and $\mathbf{u_i}$ is the unit vector of magnetization of the i-th magnetic core. $\mathbf{H}_{\text{eff}}$ is the effective

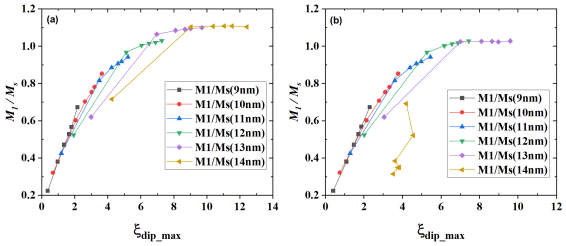

Figure 2: Effect of $\xi_{\text{dip\_max}}$ on M_1/M_s, (a) $f = 1$ kHz, (b) $f = 20$ kHz. The blue arrow represents increase of N from 2 to 20.

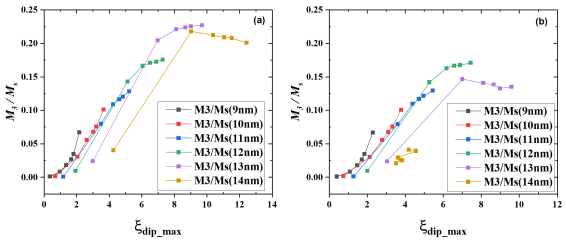

Figure 3: Effect of $\xi_{\text{dip\_max}}$ on M_3/M_s, (a) $f = 1$ kHz, (b) $f = 20$ kHz. The blue arrow represents increase of N from 2 to 20.

magnetic field given by

$$\mathbf{H}_{\text{eff},i} = \mathbf{H}_{\text{ex}} + \mathbf{H}_{\text{ani},i} + \mathbf{H}_{\text{dip},i} + \mathbf{H}_{\text{th},i}, \tag{2}$$

Here, $\mathbf{H}_{\text{ex}} = \mathbf{H}_{\text{ac}} \sin(2\pi f t)$, $\mathbf{H}_{\text{ani},i} = \frac{2K}{M_s}(\mathbf{u}_i \cdot \mathbf{n}_i)\mathbf{n}_i$, $\mathbf{H}_{\text{dip},i} = \sum_{j=1, j\neq i}^{N} \frac{1}{4\pi|\mathbf{r}_{ji}|^3}\left(\frac{3\mathbf{m}_j \cdot \mathbf{r}_{ji}}{|\mathbf{r}_{ji}|^2}\mathbf{r}_{ji} - \mathbf{m}_j\right)$. $\mathbf{H}_{\text{ex}}$ is external magnetic field, $\mathbf{H}_{\text{ani},i}$ is anisotropic magnetic field, $\mathbf{H}_{\text{dip},i}$ is the magnetic field of the dipole interaction acting on the i-th magnetic core, $|m_j| = M_s \frac{\pi}{6} d_c^3$, d_c is the diameter of the magnetic core. $\mathbf{H}_{\text{th},i}$ refers to fluctuating magnetic field generated by thermal noise.

III. Simulation results

In these simulations, we assumed that the easy axes of MNPs were fixed and aligned in the direction of $\mathbf{H}_{\text{ex}}$ (z-axis). We set the characteristic Néel rotational relaxation time $\tau_{N0} = M_s/2\gamma\lambda K = 10^{-9}$ s [4], $\lambda = 10.0$, $M_s = 400$ kA/m, $K = 10$ kJ/m^3, $\mu_0 H_{ac} = 10$ mT, and $T = 300$ K. Considering the feasibility of the actual MNPs, d_c is changed from 9-14 nm [5], and the number of magnetic core N in a CMNP is set to 2, 4, 6, 8, 10, 20 as depicted in Fig. 1. Note that the value of d_c is fixed in each simulation. Fig. 2 shows the effect of dipolar interaction on the fundamental harmonic of magnetization M_1/M_s at different AC frequency f. Here, ξ_{dip} and $\xi_{\text{dip\_max}}$ are

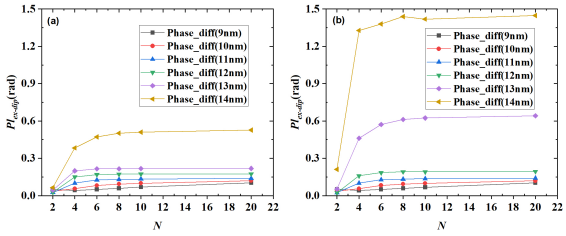

Figure 4: Pl_{ex-dip} for different d_c and N, (a) $f = 1$ kHz, (b) $f = 20$ kHz.

given by

$$\xi_{\text{dip}} = \frac{\mu_0 m \langle \mathbf{H}_{\text{dip,z}} \rangle}{k_B T} \qquad \xi_{\text{dip\_max}} = \max(\xi_{\text{dip}}). \tag{3}$$

$\langle \mathbf{H}_{\text{dip,z}} \rangle$ is the average value of z-axis component of the dipolar interaction field.

As shown in Fig. 2 (a) and (b), M_1/M_s is approximately represented by a single curve regardless of d_c. Only at $f = 20$ kHz and d_c of 14 nm, the trend of M_1/M_s deviates from others. Fig. 3 illustrates the effect of $\xi_{\text{dip\_max}}$ on the third harmonic magnetization M_3/M_s at different f. Unlike M_1/M_s, M_3/M_s is not uniquely determined by $\xi_{\text{dip\_max}}$. As shown in Fig. 3 (a), when the d_c is between 9 and 13 nm at $f = 1$ kHz, M_3/M_s increases with $\xi_{\text{dip\_max}}$, however the increase rate depends on d_c. For $d_c = 14$ nm and $N > 4$, the M_3/M_s decreases as $\xi_{\text{dip\_max}}$ increase. In Fig. 3 (b), the trend of M_3/M_s for $d_c = 13$ nm at $f = 20$ kHz is similar to that for $d_c = 14$ nm at $f = 1$ kHz. Additionally, the M_3/M_s of d_c below 13 nm at $f = 20$ kHz is basically the same as that at $f = 1$ kHz.

Fig. 4 shows the phase lag, Pl_{ex-dip}, between $\mathbf{H}_{ex}$ and $\langle H_{\text{dip,z}} \rangle$ at different f. As N and d_c increase, Pl_{ex-dip} increases, and for $d_c = 14$ nm, Pl_{ex-dip} is much larger than other small d_c. As shown in Fig. 2 (a) and Fig. 4 (a), the effect of Pl_{ex-dip} on M_1/M_s is not obvious. On the other hand, as shown in Fig. 3 (a) and Fig. 4 (a), M_3/M_s is more susceptible to Pl_{ex-dip} compared to M_1/M_s. However, when f increases to 20 kHz and $d_c = 14$ nm, as shown in Fig. 2 (b) and Fig. 4 (b), large Pl_{ex-dip} also reduce M_1/M_s.

IV. Conclusions

The simulation results showed that the third harmonic component of the magnetization is not uniquely determined by the magnitude of dipole interaction field, it is more susceptible to the phase lag between external field and dipole interaction field. Although the CMNP have stronger signal intensity than conventional MNPs for MPI [2], considering the influence of the phase difference between the dipole interaction field and the ex-

citation field on the third harmonic, CMNPs composed of MNPs with a core size greater than 13 nm should be avoided.

Acknowledgments

This work was supported in part by JSPS KAKENHI (Grant Nos. JP20H05652, JP23K20940, and JP23K17750).

Author's statement

Conflict of interest: Authors state no conflict of interest.
Informed consent: Informed consent has been obtained from all individuals included in this study.

References

[1] B. Gleich, and J. Weizenecker, *Tomographic imaging using the nonlinear response of magnetic particles*, Nature, 435, 1214-1217, 2005.

[2] Z.W. Tay, S. Savliwala, D.W. Hensley, et al. *Superferromagnetic Nanoparticles Enable Order-of-Magnitude Resolution & Sensitivity Gain in Magnetic Particle Imaging*, Small Methods, vol. 5, 2100796, 2021.

[3] W.T. Coffey, Y.P. Kalmykov, J.T. Waldron, *The Langevin Equation*, World Scientific, Singapore 95, 1996.

[4] W.T. Coffey, Y.P. Kalmykov, *Thermal fluctuations of magnetic nanoparticles: Fifty years after Brown*, Journal of Applied Physical., vol. 112, 120301, 2012.

[5] F.L. Durhuus, L.H. Wandall, M.H. Boisen, et al. *Simulated clustering dynamics of colloidal magnetic nanoparticles*, Nanoscale, vol. 13(3), pp.1970–1981, 2021.

10.18416/ijmpi.2025.2503035